

Watershed Surface and Subsurface Spatial Intraflows Model

Thomas E. Croley II¹ and Chansheng He²

Abstract: We present new developments to the original, spatially lumped large basin runoff model (LBRM) of the National Oceanic and Atmospheric Administration's Great Lakes Environmental Research Laboratory. In addition to making it a two-dimensional, spatially distributed model, we modify it to allow routing flows between adjacent cells upper soil zones, lower soil zones, and groundwater zones. We modify the LBRM continuity equations for these additional flows and add corresponding corrector terms to the original solution equations. We derive the flow network from elevation and hydrography and the LBRM automatically arranges cell computations. We apply the newly modified LBRM to the Kalamazoo River watershed in Michigan and to the Maumee River watershed in Ohio. The simulations show that the Kalamazoo River has dominant groundwater storage, allowing delayed and sustained hydrologic responses to rainfall whereas the Maumee River lacks any significant groundwater storage, allowing a fast flashy response to rainfall. These results are characteristic of the study watersheds, indicating that the addition of subsurface intraflows in the model has improved watershed representation.

DOI: 10.1061/(ASCE)1084-0699(2006)11:1(12)

CE Database subject headings: Hydrology; Watersheds; Parameters; Subsurface flow; Hydrologic models.

Introduction

Effective management of the Great Lakes water resources requires better representation and simulation of the Great Lakes hydrological systems. The National Oceanic and Atmospheric Administration's Great Lakes Environmental Research Laboratory (GLERL) has been involved in this endeavor over the past three decades. They developed their large basin runoff model (LBRM) as a serial and parallel cascade of linear reservoirs (outflows proportional to storage) representing moisture storages within a watershed: Surface, upper soil zone, lower soil zone, and groundwater zone; see Fig. 1. It computes potential evapotranspiration from a heat balance, indexed by daily air temperature, and takes actual evapotranspiration as proportional to both the potential and storage. It uses variable-area infiltration (infiltration proportional to unsaturated fraction of upper soil zone) and degree-day snowmelt. It uses daily precipitation and minimum and maximum air temperature and is calibrated in a systematic parameter search to minimize the root mean square error between modeled and observed daily watershed outflows (Croley 2002). It has been applied extensively to the 121 riverine watersheds draining into the Laurentian Great Lakes for use in both simulation (Croley and Luukkonen 2003; Croley et al. 1998; Quinn and Croley 1999) and forecasting (Croley 2005).

Recently, GLERL adapted the LBRM from its lumped-parameter definition for an entire watershed to a two dimensional

representation of the flow cells comprising the watershed (Croley and He 2005) and applied it to the Kalamazoo watershed (Croley et al. 2005). This involved changes to the model structure to apply it to the microscale as well as organization of watershed cells and an implementation of spatial flow routing. GLERL modified the LBRM continuity equations to allow upstream surface inflow when the model is applied to a single cell within a watershed and found the modifications in terms of corrector equations to be applied to the original solution. They considered flows between adjacent cells' surface storages while keeping the upper soil zone, lower soil zone, and groundwater zones in each cell independent. Thus each cell's upper soil zone, lower soil zone, and groundwater zone connected only to that cell's surface zone and not to any other cell, but the surface zones connected between adjacent cells. Such additions improve the representation and accuracy of rainfall runoff simulation since model structure has an important effect on model performance (Mohseni and Stefan 1998; Gan et al. 1997; Valeo and Moin 2001). Application of the spatially distributed LBRM to the 5,612 1-km² cells of the Kalamazoo River watershed yielded outflow errors comparable to the original lumped model, but flows in the soil zones and groundwater zone were judged unrealistic since storage there flowed only into the surface zone in each cell and not between cells.

As accurate accounting of soil water storage and spatial variation produces better runoff estimates (VanderKwaak and Loague 2001; Martinez et al. 2001; Merz and Plate 1997; Zhu and Mackay 2001), here we further modify the model to allow subsurface routing between cells of flows of the upper soil zone, the lower soil zone, and the groundwater zone. This allows surface and subsurface flows to interact both with each other and with adjacent-cell surface and subsurface storages. Such an improved model will allow tracing of water-borne materials, important in simulations of watershed movements of pesticides, fertilizers, and other agricultural materials. The modifications involve adding additional flows out of the various subsurface storages in a watershed cell and additional flows (from upstream watershed cells' subsurface storages) into the storages. The continuity equa-

¹Research Hydrologist, Great Lakes Environmental Research Laboratory, 2205 Commonwealth Blvd., Ann Arbor, MI 48105-2945.

²Professor, Dept. of Geography, Western Michigan Univ., 3234 Wood Hall, Kalamazoo, MI 49008-5424.

Note. Discussion open until June 1, 2006. Separate discussions must be submitted for individual papers. To extend the closing date by one month, a written request must be filed with the ASCE Managing Editor. The manuscript for this paper was submitted for review and possible publication on May 19, 2004; approved on March 11, 2005. This paper is part of the *Journal of Hydrologic Engineering*, Vol. 11, No. 1, January 1, 2006. ©ASCE, ISSN 1084-0699/2006/1-12-20/\$25.00.

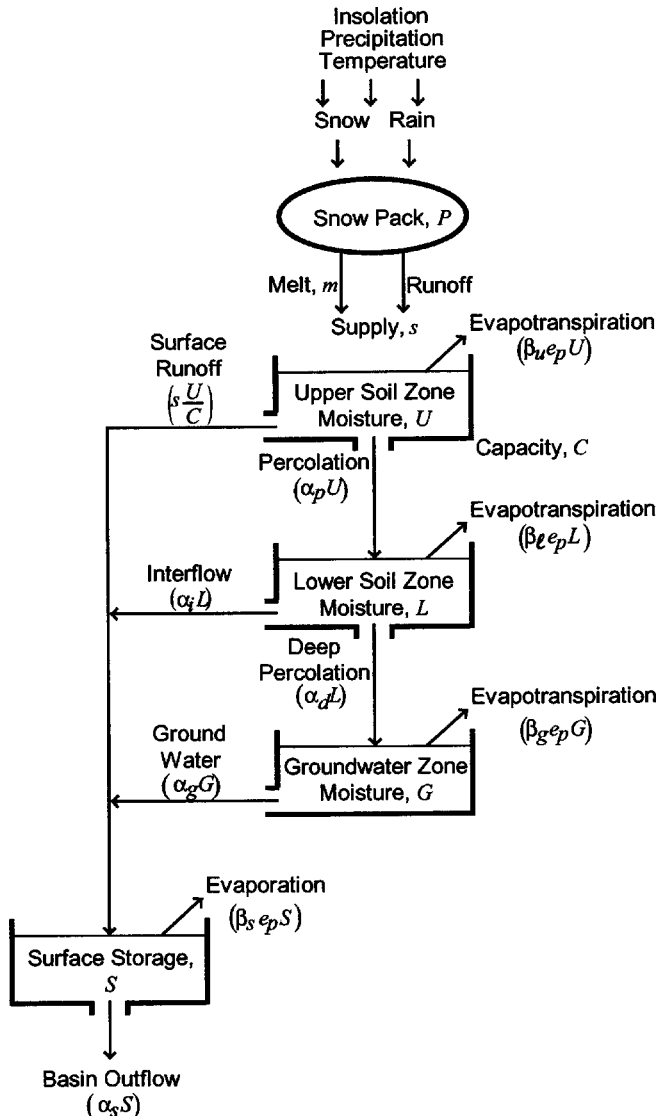


Fig. 1. LBRM tank cascade schematic

tions are again modified in terms of corrector equations applied to the original solution and are derived handily. We then organize LBRM applications to constituent watershed cells into a flow network by again identifying the network flow cascade and automatically arranging the cell computations accordingly. Finally, we apply the model to investigate alternatives and to demonstrate surface–subsurface interactions in a distributed spatial context. Currently, many large scale distributed models use state variables that represent local averages of storage or flow depths at coarse scales (e.g., at spatial resolutions ranging from 0.5° to 5° latitude and longitude) to make predictions that are distributed in space (Abdulla et al. 1996; Nijssen et al. 1997; Vörösmarty et al. 1996; Ferrari et al. 1999). Our modifications of the distributed LBRM better account for spatial variation and processes of surface runoff, interflow, groundwater, and basin outflow because we use much finer spatial resolution (1 km² cell definition); this significantly improves the representation of the watershed hydrological system over the large scale.

LBRM Structural Modification

The schematic in Fig. 1 shows the mass balance of the unmodified LBRM. Daily precipitation, temperature, and insolation (the

latter available from meteorological summaries as a function of location) are used to determine snow pack accumulations and net supply, s . The net supply is divided into surface runoff, $s(U/C)$, and infiltration to the upper soil zone, $s - s(U/C)$, in relation to the upper soil zone moisture storage, U , and the fraction it represents of the upper soil zone capacity, C (variable-area infiltration concept). Percolation to the lower soil zone, $\alpha_p U$, and evapotranspiration, $\beta_u e_p U$, are taken as outflows from a linear reservoir (flow is proportional to storage). Likewise, interflow from the lower soil zone to the surface, $\alpha_i L$, evapotranspiration, $\beta_l e_p L$, and deep percolation to the groundwater zone, $\alpha_d L$, are linearly proportional to the lower soil zone moisture content, L . Groundwater flow, $\alpha_g G$, and evapotranspiration from the groundwater zone, $\beta_g e_p G$, are linearly proportional to the groundwater zone moisture content, G . Finally, basin outflow, $\alpha_s S$, and evaporation from the surface storage, $\beta_s e_p S$, depend on its content, S . Additionally, evaporation and evapotranspiration depend on potential evapotranspiration, e_p , determined by considering available moisture and watershed heat balance.

Mass conservation equations (Croley 2002) are repeated here for convenience as differential equations with respect to time t

$$\frac{d}{dt}U = s \left(1 - \frac{U}{C} \right) - \alpha_p U - \beta_u e_p U \quad (1)$$

$$\frac{d}{dt}L = \alpha_p U - \alpha_i L - \alpha_d L - \beta_l e_p L \quad (2)$$

$$\frac{d}{dt}G = \alpha_d L - \alpha_g G - \beta_g e_p G \quad (3)$$

$$\frac{d}{dt}S = s \frac{U}{C} + \alpha_i L + \alpha_g G - \alpha_s S - \beta_s e_p S \quad (4)$$

Croley (2002) solved the equations analytically, yielding storages at the end of a time increment (U_t , L_t , G_t , and S_t) as functions of the inputs, parameters, and beginning-of-time-increment storages (storages at the end of the previous time increment: U_0 , L_0 , G_0 , and S_0) by taking net supply and potential evapotranspiration as uniform over the increment. There are no errors arising out of a numerical solution since the solution is analytic; however, the time increment should be short enough so that the assumption of uniform net supply and potential evapotranspiration is valid. Here, as in past studies with the LBRM, we use a time interval of 1 day. The surface storage solution is

$$S_t = e^{-(\alpha_s + \beta_s e_p)t} \left[S_0 + \int_0^t \left(s \frac{U}{C} + \alpha_i L + \alpha_g G \right) e^{(\alpha_s + \beta_s e_p)v} dv \right] \quad (5)$$

In all cases, we can determine outflow flow volumes directly since they are related by their ratio of linear reservoir coefficients. In particular, the volume of basin outflow is

$$V_s = (V_r + V_i + V_g + S_0 - S_t) \frac{\alpha_s}{\alpha_s + \beta_s e_p} \quad (6)$$

where V_s =basin outflow volume from surface storage; V_r =surface runoff volume; V_i =interflow volume; and V_g =groundwater volume, all into surface storage, over increment $(0, t)$.

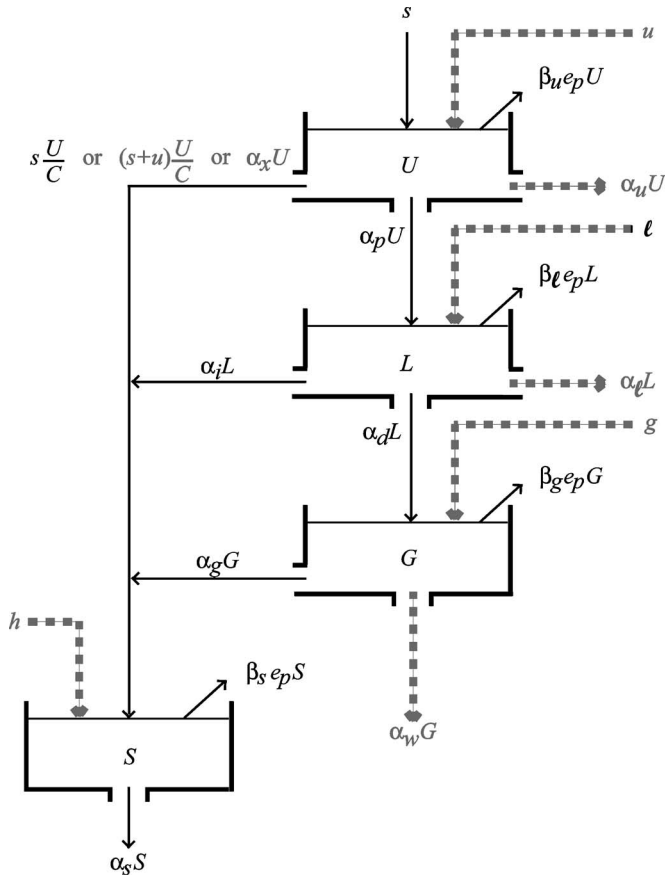


Fig. 2. LBRM with U , L , G , and S zone inflows and outflows

Upstream Surface Flow

An amended mass balance schematic for a watershed cell is shown in Fig. 2, where upstream surface flows are added (from an upstream cell). Consider first the surface zone only. The mass balance is the same employed by Croley (2002) except for adding the upstream surface flow, h . By using the above-mentioned nomenclature for the case with no upstream cell flow ($h=0$) and a “prime” notation for the case with upstream cell flow, Croley and He (2005) take h constant over the time interval and show that starting from the same initial storage, $S'_0=S_0$ at $t=0$

$$S'_t = S_t + h \frac{(1 - e^{-(\alpha_s + \beta_s e_p)t})}{\alpha_s + \beta_s e_p} \quad (7)$$

$$V'_s = V_s + h \left(t - \frac{(1 - e^{-(\alpha_s + \beta_s e_p)t})}{\alpha_s + \beta_s e_p} \right) \frac{\alpha_s}{\alpha_s + \beta_s e_p} \quad (8)$$

Therefore, the output of the LBRM, applied to a single cell with no inflow from an upstream cell, (S_t and V_s) can be corrected each time increment with Eqs. (7) and (8) to reflect the presence of an inflow, h , from an upstream cell (S'_t and V'_s). The outflow volume from the cell, V'_s , determines the inflow to the next downstream cell; again approximating it as constant over the time interval, it is determined by dividing by the time interval.

Upstream Groundwater Flow

We can similarly expand the LBRM to include upstream groundwater flows. First we must allow an additional flow out of the groundwater storage (to be passed to the downstream cell as an

upstream groundwater flow). Since the groundwater storage is represented as a linear reservoir, this additional flow will be $\alpha_w G$, where α_w =linear reservoir coefficient governing groundwater flows directly to downstream cell groundwater storages. Then we must allow an upstream flow into the groundwater storage, g ; see Fig. 2. By again using the preceding nomenclature for the case with no upstream cell flow to the groundwater storage ($g=0$), the general solution for groundwater storage from Eq. (3) is

$$G_{t,\alpha_g} = e^{-(\alpha_g + \beta_g e_p)t} \left(G_0 + \int_0^t \alpha_d L e^{(\alpha_g + \beta_g e_p)v} dv \right) \quad (9)$$

$$V_{g,\alpha_g} = (V_d + G_0 - G_{t,\alpha_g}) \frac{\alpha_g}{\alpha_g + \beta_g e_p} \quad (10)$$

where G_{t,α_g} and V_{g,α_g} =respectively, storage at the end of time increment $(0,t)$ and groundwater flow volume into surface storage, both written as a function of α_g for convenience later, and V_d =deep percolation volume into groundwater storage over increment $(0,t)$. Considering now $g \neq 0$, Eq. (3) and its solution become

$$\frac{d}{dt} G' = \alpha_d L - \alpha_g G' - \beta_g e_p G' - \alpha_w G' + g \quad (11)$$

$$G'_t = e^{-(\alpha_g + \alpha_w + \beta_g e_p)t} \left[G'_0 + \int_0^t (\alpha_d L + g) e^{(\alpha_g + \alpha_w + \beta_g e_p)v} dv \right] \quad (12)$$

If we approximate g as constant over the time interval $(0,t)$:

$$G'_t = e^{-(\alpha_g + \alpha_w + \beta_g e_p)t} \left(G'_0 + \int_0^t \alpha_d L e^{(\alpha_g + \alpha_w + \beta_g e_p)v} dv \right) + e^{-(\alpha_g + \alpha_w + \beta_g e_p)t} g \int_0^t e^{(\alpha_g + \alpha_w + \beta_g e_p)v} dv \quad (13)$$

Now, for $G'_0=G_0$ at $t=0$, we have

$$G'_t = G_{t,\alpha_g + \alpha_w} + g \frac{1 - e^{-(\alpha_g + \alpha_w + \beta_g e_p)t}}{\alpha_g + \alpha_w + \beta_g e_p} \quad (14)$$

$$\begin{aligned} V'_g + V'_w &= V'_{g+w} \\ &= (V_d + G'_0 - G'_t + gt) \frac{\alpha_g + \alpha_w}{\alpha_g + \alpha_w + \beta_g e_p} \\ &= V_{g,\alpha_g + \alpha_w} + g \left(t - \frac{1 - e^{-(\alpha_g + \alpha_w + \beta_g e_p)t}}{\alpha_g + \alpha_w + \beta_g e_p} \right) \frac{\alpha_g + \alpha_w}{\alpha_g + \alpha_w + \beta_g e_p} \end{aligned} \quad (15)$$

where the subterranean outflow volume, V'_w , from groundwater storage ($V'_w = [\alpha_w / (\alpha_g + \alpha_w)] V'_{g+w}$) determines the groundwater inflow to the next downstream cell. Again, approximating it as constant over the time interval, it is determined by dividing by the length of the time interval. Therefore, existing computer code in the LBRM encoding can be applied for upstream groundwater flow, g , into the groundwater storage by substituting $\alpha_g + \alpha_w$ for α_g in Eqs. (9) and (10) and correcting each time increment with Eqs. (14) and (15). The outflow volume from the cell's groundwater storage, $V'_g = V'_{g+w} - V'_w$, would be used (as V_g) in Eq. (6) to compute the basin outflow volume, V_s , which is then used in Eq. (8) to compute the corrected basin outflow volume, V'_s .

Other Storage Upstream Flows

We can also similarly expand the LBRM to include other flows into the upper and lower soil zone storages from respective upstream cells' storages; see Fig. 2. Again, first we must allow an additional flow out of each storage (to be passed to the downstream cell's respective storage as an upstream flow). Since the storages are represented as linear reservoirs, these additional flows will be $\alpha_u U$ and $\alpha_\ell L$, respectively, from the upper and lower soil zone moisture storages, where α_u and α_ℓ are the linear reservoir coefficients. Then we must allow upstream flows, u and ℓ , into these storages, respectively. By again using the original nomenclature for the case with no upstream cell flow to the upper or lower soil zone moisture storages, the general solution for each can be found in terms of function definitions already coded and corrector equations as was the case for the groundwater storage. They are derived and defined similarly; for the upper soil zone

$$U_{t,s} = e^{-(s/C + \alpha_p + \beta_u e_p)t} \left(U_0 + \int_0^t s e^{(s/C + \alpha_p + \beta_u e_p)v} dv \right) \quad (16)$$

$$V_{r,s} = (st + U_0 - U_{t,s}) \frac{\frac{s}{C}}{\frac{s}{C} + \alpha_p + \beta_u e_p} \quad (17)$$

$$U'_t = U_{t,s + \alpha_u C} + (u - \alpha_u C) \frac{1 - e^{-(s/C + \alpha_u + \alpha_p + \beta_u e_p)t}}{\frac{s}{C} + \alpha_u + \alpha_p + \beta_u e_p} \quad (18)$$

$$\begin{aligned} V'_r + V'_u &= V'_{r+u} = V_{r,s + \alpha_u C} + (u - \alpha_u C) \\ &\times \left(t - \frac{1 - e^{-(s/C + \alpha_u + \alpha_p + \beta_u e_p)t}}{\frac{s}{C} + \alpha_u + \alpha_p + \beta_u e_p} \right) \\ &\times \frac{\frac{s}{C} + \alpha_u}{\frac{s}{C} + \alpha_u + \alpha_p + \beta_u e_p} \end{aligned} \quad (19)$$

where the subterranean outflow volume, $V'_u = \alpha_u / (s/C + \alpha_u) V'_{r+u}$, from the upper soil zone storage determines the upper soil zone inflow to the next downstream cell. Again, approximating it as constant over the time interval, it is determined by dividing by the length of the time interval. Existing computer code in the LBRM encoding can be applied for upstream flow into the upper soil zone, u , by substituting $s + \alpha_u C$ for s in Eqs. (16) and (17) and correcting each time increment with Eqs. (18) and (19). The outflow volume from the cell's upper soil zone storage, $V'_r = V'_{r+u} - V'_u$, would be used (as V_r) in Eq. (6) to compute the basin outflow volume, V_s , which is then used in Eq. (8) to compute the corrected basin outflow volume, V'_s .

We can show that the upper soil zone moisture in Eq. (18) is no longer bound by C (as an upper limit) as it is in Eq. (16). That means that supply infiltration, $s - s(U/C)$, can be negative unless C is sufficiently large. This can be a problem for some of the most-downstream cells in a watershed since upstream upper soil zone flow can be accumulated to large levels. Alternatively, the additional flow out of the upper soil zone into the surface zone, due to the addition of the upstream flow, u , could be governed by the partial-area concept similar to the supply (s and $s(U/C)$);

it would become $u(U/C)$. Managed in this way, the upper soil zone moisture storage, U , never exceeds its capacity, C , and the solution is

$$U'_t = U_{t,s + \alpha_u C} - \alpha_u C \frac{1 - e^{-(s + u/C + \alpha_p + \alpha_u + \beta_u e_p)t}}{\frac{s + u}{C} + \alpha_p + \alpha_u + \beta_u e_p} \quad (20)$$

$$\begin{aligned} V'_{r+u} &= V_{r,s + \alpha_u C} - \alpha_u C \\ &\times \left(t - \frac{1 - e^{-(s + u/C + \alpha_p + \alpha_u + \beta_u e_p)t}}{\frac{s + u}{C} + \alpha_p + \alpha_u + \beta_u e_p} \right) \\ &\times \frac{\frac{s + u}{C} + \alpha_u}{\frac{s + u}{C} + \alpha_p + \alpha_u + \beta_u e_p} \end{aligned} \quad (21)$$

and $V'_u = \alpha_u / [(s + u)/C + \alpha_u] V'_{r+u}$. As a third alternative, we could eliminate the upper soil zone capacity variable (C) entirely, thereby considering the upper soil zone tank unbounded, as is done with the other tanks. The surface runoff and downstream upper soil zone flow would be, respectively, $\alpha_x U$ and $\alpha_u U$. The solution is

$$U'_t = U_{t,(\alpha_x + \alpha_u)C} + [s + u - (\alpha_x + \alpha_u)C] \frac{1 - e^{-(\alpha_x + \alpha_u + \alpha_p + \beta_u e_p)t}}{\alpha_x + \alpha_u + \alpha_p + \beta_u e_p} \quad (22)$$

$$\begin{aligned} V'_{r+u} &= V_{r,(\alpha_x + \alpha_u)C} + (s + u - (\alpha_x + \alpha_u)C) \\ &\times \left(t - \frac{1 - e^{-(\alpha_x + \alpha_u + \alpha_p + \beta_u e_p)t}}{\alpha_x + \alpha_u + \alpha_p + \beta_u e_p} \right) \frac{\alpha_x + \alpha_u}{\alpha_x + \alpha_u + \alpha_p + \beta_u e_p} \end{aligned} \quad (23)$$

and $V'_u = [\alpha_u / (\alpha_x + \alpha_u)] V'_{r+u}$. The upper soil zone capacity, C , drops out when Eqs. (22) and (23) are applied to Eqs. (16) and (17).

For the lower soil zone

$$L_{t,\alpha_i} = e^{-(\alpha_i + \alpha_d + \beta_\ell e_p)t} \left(L_0 + \int_0^t \alpha_p U e^{(\alpha_i + \alpha_d + \beta_\ell e_p)v} dv \right) \quad (24)$$

$$V_{i,\alpha_i} = (V_p + L_0 - L_{t,\alpha_i}) \frac{\alpha_i}{\alpha_i + \alpha_d + \beta_\ell e_p} \quad (25)$$

$$L'_t = L_{t,\alpha_i + \alpha_\ell} + \ell \frac{1 - e^{-(\alpha_i + \alpha_\ell + \alpha_d + \beta_\ell e_p)t}}{\alpha_i + \alpha_\ell + \alpha_d + \beta_\ell e_p} \quad (26)$$

$$\begin{aligned} V'_i + V'_\ell &= V'_{i+\ell} = V_{i,\alpha_i + \alpha_\ell} + \ell \left(t - \frac{1 - e^{-(\alpha_i + \alpha_\ell + \alpha_d + \beta_\ell e_p)t}}{\alpha_i + \alpha_\ell + \alpha_d + \beta_\ell e_p} \right) \\ &\times \frac{\alpha_i + \alpha_\ell}{\alpha_i + \alpha_\ell + \alpha_d + \beta_\ell e_p} \end{aligned} \quad (27)$$

where V_p = percolation volume of supply to the lower soil zone (from the upper soil zone) and the subterranean outflow volume, $V'_\ell = [\alpha_\ell / (\alpha_i + \alpha_\ell)] V'_{i+\ell}$, from the lower soil zone storage determines the lower soil zone inflow to the next downstream cell. Again, approximating it as constant over the time interval, it is determined by dividing by the length of the time interval. Existing computer code in the LBRM encoding can be applied for upstream flow into the lower soil zone, ℓ , by substituting $\alpha_i + \alpha_\ell$ for α_i in Eqs. (24) and (25) and correcting each time increment with

Eqs. (26) and (27). The interflow volume from the cell's lower soil zone storage, $V'_i = V'_{i+\ell} - V'_\ell$, would be used (as V_i) in Eq. (6) to compute the basin outflow volume, V_s , which is then used in Eq. (8) to compute the corrected basin outflow volume, V'_s .

Flow Network

Each cell in a watershed has flows from its surface and subsurface components into its surface storage, and it has flows from upstream cells into its surface storage and into its subsurface storages (except for the most-upstream cells). The association of each cell with its adjacent upstream cells, taken from drainage maps derived from elevation maps, defines the flow network. Croley and He (2005) discuss in detail how this network is created in the model and how it relates to the natural channels in the watershed. Here the surface and subsurface flow networks are taken as identical. Croley and He (2005) discuss general requirements for such networks and present a microhydrology computation-ordering algorithm for application to a well-defined flow network to order cell hydrograph and routing computations. At each cell, it sums all tributary inflows from each zone to determine the total input hydrographs into each of the storage zones of the current cell. Then it routes by solving the mass continuity equations for every time interval in the hydrographs; the original model computer code is used with altered parameters in Eqs. (5) and (6), (9) and (10), (16) and (17), and (24) and (25), and corrections are made with Eqs. (7) and (8), (14) and (15), (18) and (19), [or (20) and (21) and (23)], and (26) and (27), respectively. Finally, it assembles an outflow hydrograph from each storage for the current cell.

Application

We used a lumped-parameter calibration procedure in a distributed-parameter setting as detailed elsewhere (Croley et al. 2005) to optimize the spatial-average values of all parameters while imposing a spatial structure onto each parameter over the cells of the watershed. [The procedure minimized root mean square error between observed and modeled daily basin outflow by using a gradient search of the parameter space; the search consists of minimizing the root mean square error for each parameter, selected in rotation, until convergence in all parameters to three significant figures is achieved; for details see Croley (2002).] Although parameters describing the degree-day snow-melt and heat available for evapotranspiration were taken as spatially constant, and while β_s and β_g were taken as zero, the spatial structures of other parameters were assigned as follows:

$$(\alpha_p)_i = \bar{\alpha}_p f(K_i^U, 80\%) \quad (28)$$

$$(\beta_u)_i = \bar{\beta}_u f(K_i^U, 80\%) \quad (29)$$

$$(\alpha_i)_i = \bar{\alpha}_i f(K_i^L, 80\%) \quad (30)$$

$$(\alpha_d)_i = \bar{\alpha}_d f(K_i^L, 80\%) \quad (31)$$

$$(\beta_\ell)_i = \bar{\beta}_\ell f(K_i^L, 80\%) \quad (32)$$

$$(\alpha_g)_i = \bar{\alpha}_g f(K_i^L, 80\%) \quad (33)$$

$$(\alpha_s)_i = \bar{\alpha}_s f\left(\frac{\sqrt{s_i}}{\eta}, 80\%\right) \quad (34)$$

$$(\alpha_u)_i = \bar{\alpha}_u f(K_i^U, 80\%) \quad (35)$$

$$(\alpha_\ell)_i = \bar{\alpha}_\ell f(K_i^L, 80\%) \quad (36)$$

$$(\alpha_w)_i = \bar{\alpha}_w f(K_i^L, 80\%) \quad (37)$$

$$(C)_i = \bar{C} f(C_i^U, 80\%) \quad (38)$$

$$f(x_i, \varepsilon) = \left(\frac{x_i}{\frac{1}{n} \sum_{j=1}^n x_j} - 1 \right) \frac{\varepsilon}{100\%} + 1 \quad (39)$$

where $(\alpha)_i$ =linear reservoir coefficient for cell i ; $\bar{\alpha}_s$ =spatial average value of linear reservoir coefficient (from parameter calibration); $(\beta)_i$ and $\bar{\beta}$, are defined similarly for partial linear reservoir coefficients (used in evapotranspiration); $(C)_i$ and \bar{C} are defined similarly for the upper soil zone capacity; K_i^U =upper and K_i^L =lower soil zone permeability in cell i ; s_i =slope of cell i ; η =Manning's roughness coefficient; C_i^U =upper soil zone available water capacity; x_i =data value for cell i ; and n =number of cells in the watershed.

Kalamazoo Watershed

Croley et al. (2005) present maps of the necessary descriptors for the Kalamazoo River watershed, an agriculturally dominated watershed with a drainage area of 5,612 km² in southwestern Michigan. The model was applied at 1 km² resolution ($n=5,612$) and a daily time step by calibrating to the 1948–1964 data set of daily meteorology and watershed outflow; the first two years were used only for initialization of the model and the last 15 years were used to compare model and actual outflows. We found slightly better calibrations by using meteorology spatially interpolated for every square kilometer in the watershed by inverse squared distance from each station. Several model variations were considered, corresponding to the variations shown for upper soil zone (USZ) in Eqs. (18) and (19) [the supply entering USZ storage is affected by relative storage content (variable-area infiltration)], Eqs. (20) and (21) (both the supply and the upstream USZ flow entering storage are affected by relative storage), and Eqs. (22) and (23) [neither the supply nor the upstream USZ flow entering storage are affected by relative storage (unconstrained storage)]. As expected, the model with both the supply and the upstream USZ flow entering storage affected by relative storage, as in Eqs. (20) and (21), proved superior (lowest calibrated root mean square error). For the 1950–1965 period, the coefficient of determination (squared correlation) between model and observed watershed outflows was 0.77; the root mean square error was 0.19 mm/day (compare with a mean flow of 0.78 mm/day); the ratio of model to actual mean flow was 1.00; and the ratio of model to actual flow standard deviation was 0.87. [Croley et al. (2005) report that the lumped parameter model Kalamazoo calibration gave a root mean square error of 0.18 mm/day and the previous best-distributed model (only surface flows across cell boundaries) gave 0.22 mm/day]. Additionally, we experimented with several alternatives to the set of observations used for the spatial variation of model parameters presented in Eqs. (28)–(38). These included spatially constant values for both the USZ capacity and evapora-

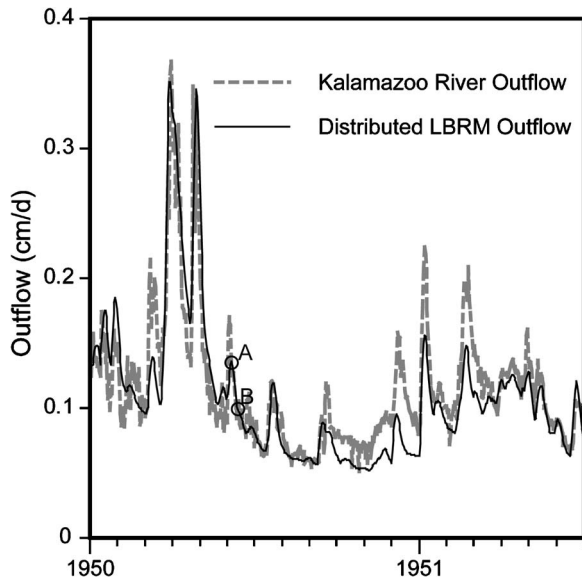


Fig. 3. Kalamazoo hydrograph comparison, 1950–1952

tion parameters; the spatial variations of Eqs. (28)–(38) proved superior, although there are several alternatives left to investigate.

Immediately apparent in a model water balance for the Kalamazoo is the absence of storage in the lower soil zone. Remember, these storage zones are conceptual only, representing multiple response functions to rainfall: the upper zone is quickest to respond and the groundwater zone is slowest. The absence of a lower zone (midspeed response) implies only two responses could be discerned in the data. Conceptually, the groundwater zone receives its input directly from the upper zone. Groundwater flow forms the majority of the outflow; there is a small groundwater flow out of the watershed, which is not part of the streamflow. Fig. 3 compares observed watershed outflow with the model for January 1950–June 1951; this period was chosen as typical of model-data agreement over the entire period (1950–1964) for both the Kalamazoo (and later the Maumee) watershed. The base flow seems well represented but several peak flows are underestimated. Fig. 4 shows the Kalamazoo watershed spatial response for recession AB in Fig. 3 (June 2–5, 1950). The ranges shown in Fig. 4 do not correspond to maximums but were chosen for best illustration of watershed response. For example, the

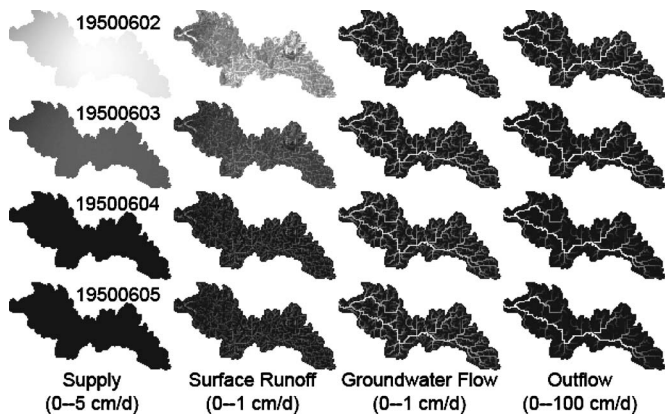


Fig. 4. Distributed large basin runoff model output for the Kalamazoo watershed

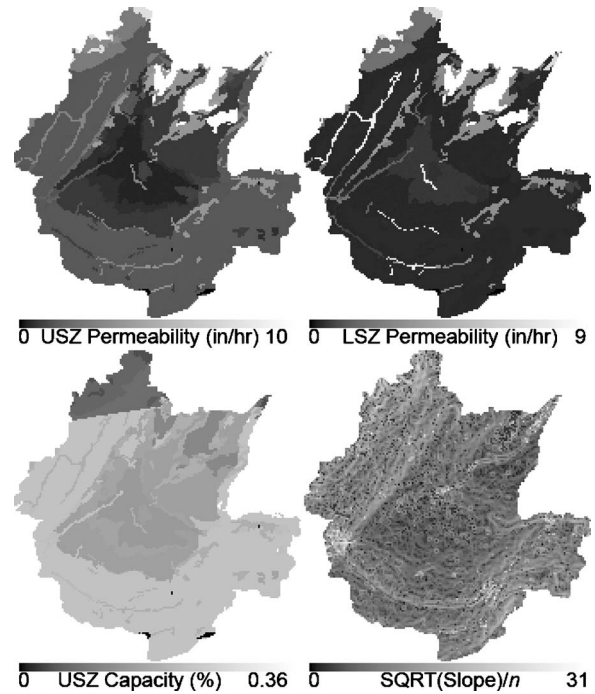


Fig. 5. Selected Maumee watershed descriptors

maximum Kalamazoo model outflow between 1948 and 1964 is about 2,000 cm/day over the last cell's 1 km² surface area (231 m³ s⁻¹) but only the range of 0–100 cm/day (0–11.6 m³ s⁻¹) is shown to emphasize the lower flows [flows above 100 cm/day (11.6 m³ s⁻¹) are shown at the same brilliance as 100 cm/day (11.6 m³ s⁻¹)]. Fig. 4 shows the watershed supply; the supply is near 5 cm/day on the first day and quickly goes to zero by Day 3. Fig. 4 also shows a flow out of each of the active storages: surface runoff flows out of the upper soil zone into the surface zone, groundwater flows from the groundwater flow zone to the surface, and outflow flows from the surface zone. Thus these flows represent the moisture storages within the watershed. The first two flows are within-the-cell flows

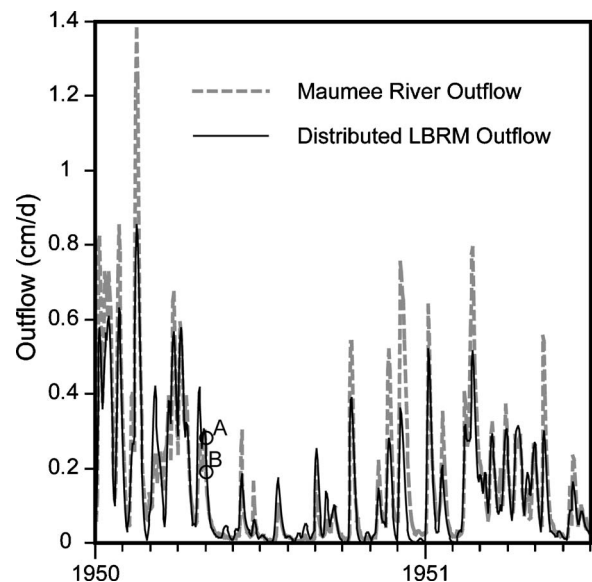


Fig. 6. Maumee hydrograph comparison, 1950–1952

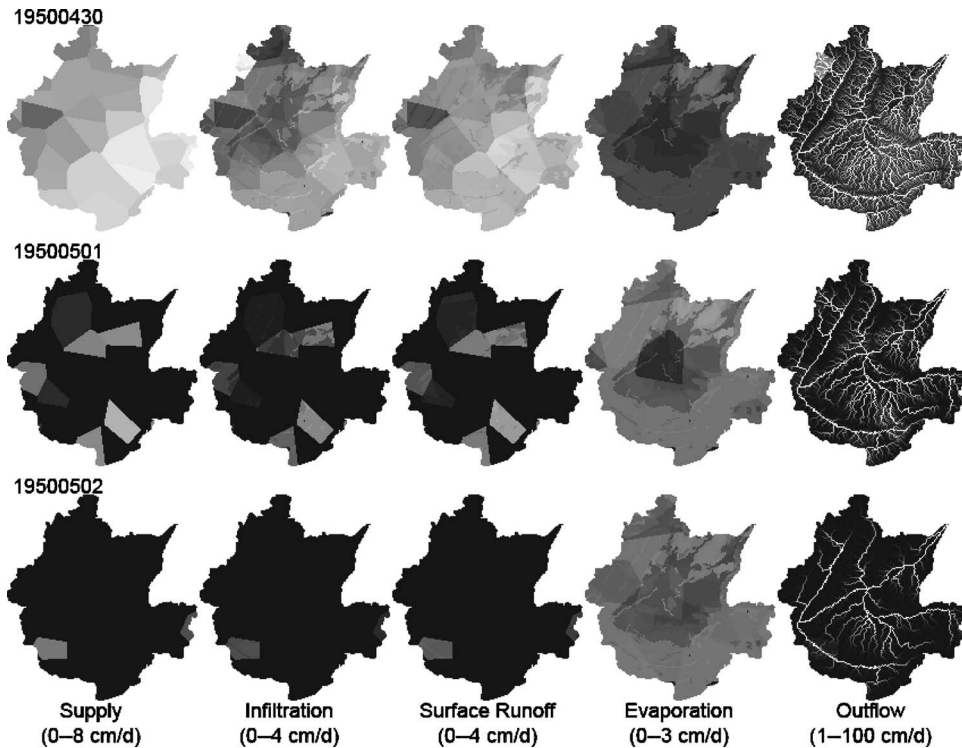


Fig. 7. Distributed large basin runoff model output for the Maumee watershed

whereas the last crosses cell boundaries and is accumulated down the flow network, reaching much larger values than within-the-cell flows. The general behavior of the watershed is depicted in this example. The supply on the first day results in a very flashy response in the upper soil zone, as seen by the immediate response in surface runoff. The groundwater zone is little affected and the groundwater flow is seen to be very nearly constant throughout the period. The surface response lies in between; the outflow network is more dense at the beginning than at the end as water flows through the network throughout the period. This strong groundwater component is characteristic to the Kalamazoo outflow and recognized from other studies, such as a hydrologic study of the Kalamazoo River by Allen et al. (1972), who found that sand and gravel with a high conductivity rate occupy much of the aquifer, and a groundwater study by Croley and Luukkonen (2003).

Maumee Watershed

The Maumee River is the largest tributary to Lake Erie, with a drainage area of 17,541 km², draining portions of northern Ohio, eastern Indiana, and southeast Michigan. Fig. 5 shows maps of Maumee watershed descriptors necessary for defining the spatial model parameter variations of Eqs. (28)–(38). Note in the map for USZ capacity in Fig. 5 that the northern-most part of the watershed is distinctly different from the rest of the watershed. The demarcation between the two parts follows the Michigan-Ohio state boundary and is related to differences in definitions used in soil maps in the two states. These differences were not resolved further here and the data sets were used as they appear in Fig. 5. The model was applied at 1 km² resolution ($n=17,541$) and a daily time step by again calibrating to a 1948–1964 data set of daily meteorology and watershed outflow in the same manner as used with the Kalamazoo calibration. We found slightly better

calibrations by using meteorology for every square kilometer in the watershed the same as the nearest station [Thiessen (Croley and Hartmann 1985)]. Again, the model with both the supply and the upstream USZ flow entering storage affected by relative storage, as in Eqs. (20) and (21), was adopted. For the 1950–1964 period, the coefficient of determination (squared correlation) between model and observed watershed outflows was 0.83; the root mean square error was 0.56 mm/day (compare with a mean flow of 0.79 mm/day); the ratio of model to actual mean flow was 1.08; and the ratio of model to actual flow standard deviation was 0.84. The lumped parameter model Maumee calibration gave 0.77 determination coefficient and 0.63 mm/day root mean square error. Thus, for the Maumee, the distributed model provides better lumped statistics than the lumped model; the Maumee watershed is large enough to allow the distributed model to capture significant spatial variations.

Immediately apparent in a model simulation of the Maumee is the absence of moisture storage response for other than the upper soil zone. The watershed soil zone moisture storage is apparent only as a one-layer system consisting of the upper soil zone. Fig. 6 compares observed outflow with the model for January 1950–June 1951, showing generally good agreement. The model underestimates most of the peak flows but over-estimates as many of the small peak flows as it underestimates. Fig. 7 shows the Maumee watershed spatial response for recession AB in Fig. 6 (April 30–May 2, 1950). Since Thiessen weighting was used to reduce meteorological station data over the Maumee watershed, the Thiessen-polygonal pattern is evident in several of the plots in Fig. 7. One can also discern patterns related to the soil parameter structures shown in Fig. 5, including the northern demarcation between Ohio and Michigan. Since soil moisture storage occurs in the model only in the upper soil zone, upper soil zone attributes are mostly shown. Most of the supply occurs on the first day of

the sequence in Fig. 7 and both infiltration and surface runoff mirror its spatial distribution (both on that day and on later days with spotty supplies). Evaporation appears maximum on the last day of the sequence. Surface response is indicated by the outflow plots and shows maximum response at the beginning with a well-defined recession apparent over the remaining days in the sequence. The absence of groundwater response is consistent with the hydrology of the Maumee (USEPA 2003; USGS 2003). The Maumee model application has only one lateral (upstream-downstream) component: surface outflow; there are no flows between cells of upper soil zone, lower soil zone, or groundwater zone. Therefore, only the surface exhibits a hierarchy of drainage (as shown in Fig. 7); the other zones show no such hierarchy (no cells flow into others).

Summary

GLERL's LBRM continuity equations were modified to allow upstream inflows when the model is applied to a single cell within a watershed. The LBRM is now applied, in both spatial dimensions, to a system of cells comprising a watershed. The inflows to each cell can now consist of outflows from upstream surface storages, upper soil zones, lower soil zones, and groundwater zones. The outflows from a cell consist of similar flows from the cell's own moisture storage zones. The modifications to the LBRM were devised in terms of both the original continuity equations (with no upstream/downstream flows) with new parameters (so we can use the same computer code) and new corrector equations to be applied to the original equation solution. LBRM applications to constituent watershed cells are organized in a flow network by identifying the network flow cascade and then automatically arranging the cell computations accordingly.

Calibration consists of finding the spatial means of 15 model parameters that best minimize the root mean square error between observed and modeled daily watershed outflows, while fixing spatial variation of each parameter to match that of selected observable watershed characteristics. We used upper and lower soil zone permeabilities, the upper soil zone available water capacity, and the square root of surface slope divided by Manning's roughness coefficient. Application was made to the Kalamazoo River watershed in Michigan and to the Maumee River watershed in Ohio. The former is recognized as having a strong base flow component while the latter is not. The model calibrations yielded behavior consistent with these observations. The Kalamazoo was found to have a groundwater storage that dominates the surface flow, allowing delayed hydrograph response to rainfall, whereas the Maumee was found to lack any significant groundwater storage; its response to rainfall is governed rather by the very large (spatially) surface network. Better understanding of the model application to these watersheds waits on comparisons of model intraflows to flow data at points interior to each watershed.

Acknowledgment

This is GLERL contribution No. 1311.

Notation

The following symbols were used in this paper:

- \bar{C} = spatial average value of upper soil zone capacity;
- C = upper soil zone capacity;
- $(C)_i$ = upper soil zone capacity for cell i ;
- C_i^U = available upper soil zone water capacity from soil survey;
- e_p = potential evapotranspiration rate;
- G = groundwater storage with no upstream groundwater flow;
- G' = groundwater storage with an upstream groundwater flow;
- g = upstream groundwater flow;
- h = upstream surface flow;
- K_i^L = lower soil zone permeability in cell i ;
- K_i^U = upper soil zone permeability in cell i ;
- L = lower soil zone storage with no upstream lower soil zone flow;
- L' = lower soil zone storage with an upstream lower soil zone flow;
- ℓ = upstream lower soil zone flow;
- n = number of cells in the watershed;
- S = surface storage with no upstream surface flow;
- S' = surface storage with an upstream surface flow;
- s = net supply;
- s_i = slope of cell i ;
- t = time;
- U = upper soil zone storage with no upstream upper soil zone flow;
- U' = upper soil zone storage with an upstream upper soil zone flow;
- u = upstream upper soil zone flow;
- V_d = daily deep percolation volume;
- V_g = daily groundwater flow volume with no upstream groundwater flow;
- V_g' = daily groundwater flow volume with an upstream groundwater flow;
- V_{g+w}' = daily sum of groundwater and downstream groundwater flow volumes;
- V_i = daily interflow volume with no upstream lower soil zone flow;
- V_i' = daily interflow volume with an upstream lower soil zone flow;
- $V_{i+\ell}'$ = daily sum of interflow and downstream lower soil zone flow volumes;
- V_p = daily percolation volume;
- V_r = daily surface runoff volume with no upstream upper soil zone flow;
- V_r' = daily surface runoff volume with an upstream upper soil zone flow;
- V_{r+u}' = daily sum of surface runoff and downstream upper soil zone flow volumes;
- V_s = daily surface outflow volume with no upstream surface flow;
- V_s' = daily surface outflow volume with an upstream surface flow;
- V_u' = daily downstream upper soil zone flow volume;

V'_w = daily downstream groundwater flow volume;
 x_i = data value for cell i ;
 α_d = deep percolation coefficient;
 α_g = groundwater flow coefficient;
 α_i = interflow coefficient;
 α_ℓ = coefficient for downstream lower soil zone flow;
 α_p = percolation coefficient;
 α_s = basin outflow coefficient;
 α_u = coefficient for downstream upper soil zone flow;
 α_w = coefficient for downstream groundwater flow;
 α_x = coefficient for surface runoff;
 $\bar{\alpha}$ = spatial average value of linear reservoir coefficient;
 $(\alpha)_i$ = linear reservoir coefficient for cell i ;
 β_g = groundwater zone evapotranspiration coefficient;
 β_ℓ = lower soil zone evapotranspiration coefficient;
 β_s = surface storage evaporation coefficient;
 β_u = upper soil zone evapotranspiration coefficient;
 $\bar{\beta}$ = spatial average value of partial linear reservoir coefficient;
 $(\beta)_i$ = partial linear reservoir coefficient for cell i ; and
 η = Manning's roughness coefficient.

References

- Abdulla, F. A., Lettenmaier, D. P., Wood, E. F., and Smith, J. A. (1996). "Application of a macroscale hydrologic model to estimate the water balance of the Arkansas-Red River Basin." *J. Geophys. Res.* 101(D3), 7449–7459.
- Allen, W. B., Miller, J. B., and Wood, W. W. (1972). "Availability of water in Kalamazoo County, Southwestern Michigan." *U.S. Geological Survey Water-Supply Paper 1973*, U.S. Government Printing Office, Washington, D.C.
- Croley, T. E., II. (2002). "Large basin runoff model." *Mathematical models in watershed hydrology*, Water Resources Publications, Littleton, Colo., 717–770.
- Croley, T. E., II. (2005). "Great Lakes advanced hydrologic prediction system." *ASCE Task Committee Rep. on Climatic Variability, Climate Change, and Water Resources Management*, J. Garbrecht and U. Lall, eds., ASCE, Arlington, Va., in press.
- Croley, T. E., II, and Hartmann, H. C. (1985). "Resolving Thiessen polygons." *J. Hydrol.*, 76(3/4), 363–379.
- Croley, T. E., II, and He, C. (2005). "Distributed-parameter Large Basin Runoff Model I: Model development." *J. Hydrologic Eng.*, 10(3), 173–181.
- Croley, T. E., II, He, C., and Lee, D. H. (2005). "Distributed-parameter Large Basin Runoff Model. II: Application." *J. Hydrologic Eng.*, 10(3), 182–191.
- Croley, T. E., II, and Luukkonen, C. L. (2003). "Potential climate change impacts on Lansing, Michigan ground water." *J. Am. Water Resour. Assoc.*, 39(1), 149–163.
- Croley, T. E., II, Quinn, F. H., Kunkel, K. E., and Changnon, S. J. (1998). "Great Lakes hydrology under transposed climates." *Clim. Change*, 38, 405–433.
- Ferrari, M. R., Miller, J. R., and Russell, G. R. (1999). "Modeling the effect of wetlands, flooding, and irrigation on river flow: Application to the Aral Sea." *Water Resour. Res.*, 35(6), 1869–1876.
- Gan, T. Y., Dlamini, E. M., and Biftu, G. F. (1997). "Effects of model complexity and structure, data quality, and objective functions on hydrologic modeling." *J. Hydrol.*, 192(1997), 81–103.
- Martinez, J. E., Dunchon, C. E., and Crosson, W. L. (2001). "Effect of the number of soil layers on a modeled surface water budget." *Water Resour. Res.*, 37(2), 367–377.
- Merz, B., and Plate, E. J. (1997). "An analysis of the effects of spatial variability of soil and soil moisture on runoff." *Water Resour. Res.*, 33(12), 2909–2922.
- Mohseni, O., and Stefan, H. J. (1998). "A monthly streamflow model." *Water Resour. Res.*, 34(5), 1287–1298.
- Nijssen, B., Lettenmaier, D. P., Liang, X., Wetzel, S. W., and Wood, E. F. (1997). "Streamflow simulation for continental-scale river basins." *Water Resour. Res.*, 33(4), 711–724.
- Quinn, F. H., and Croley, T. E., II. (1999). "Potential climate change impacts on Lake Erie." *State of Lake Erie (SOLE)—Past, Present and Future*, M. Munawar, T. Edsall, and I. F. Munawar, eds., Ecovision World Monograph Series, Backhuys, Leiden, The Netherlands, 23–30.
- United States Environmental Protection Agency (USEPA). (2003). "Maumee River area of concern. Available online at (<http://www.epa.gov/glnpo/aoc/maumee.html>) (Oct. 30, 2005).
- United States Geological Survey (USGS). (2003). "Estimated water use in the United States in 1995, counties and watersheds." available online at (<http://water.usgs.gov/watuse/spread95.html>).
- Valeo, C., and Moin, S. M. A. (2001). "Hortonian and variable source area modeling in urbanizing basins." *J. Hydrologic Eng.*, 6(4), 328–335.
- VanderKwaak, J. E., and Loague, K. (2001). "Hydrologic-response simulations for the R-5 catchment with a comprehensive physics-based model." *Water Resour. Res.*, 37(4), 999–1013.
- Vörösmarty, C. J., Willmott, C. J., Choudhury, B. J., Schloss, A. L., Stearns, T. K., Robeson, S. M., and Dorman, T. J. (1996). "Analyzing the discharge regime of a large tropical river through remote sensing. Ground-based climatic data and modeling." *Water Resour. Res.*, 32(10), 3137–3150.
- Zhu, A. X., and Mackay, D. S. (2001). "Effects of spatial detail of soil information on watershed modeling." *J. Hydrol.*, 248(1), 54–77.